Low-dose X-ray irradiation induces morphological changes and cytoskeleton reorganization in osteoblasts

QUN HUANG[1*], ZHIPING ZHOU[1*], FEI YAN[1*], QIRONG DONG[2*], LIMING WANG[1], WEIPING SHA[1], QIN XU[1], XIANWEI ZHU[1] and LEI ZHAO[1]

[1]Department of Orthopedics, The First People's Hospital of Zhangjiagang City, Suzhou, Jiangsu 215600; [2]Department of Orthopedics, The Second Affiliated Hospital of Soochow University, Suzhou, Jiangsu 215004, P.R. China

Received August 19, 2019; Accepted May 15, 2020

DOI: 10.3892/etm.2020.9413

Abstract. Recently, research into the biological effects of low dose X-ray irradiation (LDI) has been a focus of interest. Numerous studies have suggested that cells exhibit different responses and biological effects to LDI compared with high doses. Preliminary studies have demonstrated that LDI may promote osteoblast proliferation and differentiation *in vitro*, thereby accelerating fracture healing in mice. However, the exact mechanism of action by which LDI exerts its effects remains unclear. Previous studies using microarrays revealed that LDI promoted the expression of genes associated with the cytoskeleton. In the current study, the effect of X-ray irradiation (0.5 and 5 Gy) on the morphology of MC3T3-E1 cells and fiber actin organization was investigated. Osteoblasts were treated with 0, 0.5 and 5 Gy X- ray irradiation, following which changes in the actin cytoskeleton were observed. The levels of RhoA, ROCK, cofilin and phosphorylated-cofilin were measured by reverse transcription-quantitative PCR and western blotting. Subsequently, osteoblasts were pretreated with ROCK specific inhibitor Y27632 to observe the changes of actin skeleton after X-ray irradiation. The results demonstrated that the cellular morphological changes were closely associated with radiation dose and exposure time. Furthermore, the gene expression levels of small GTPase RhoA and its effectors were increased following LDI. These results indicated that the RhoA/Rho-associated kinase pathway may serve a significant role in regulating LDI-induced osteoblast cytoskeleton reorganization.

Correspondence to: Dr Fei Yan, Department of Orthopedics, The First People's Hospital of Zhangjiagang City, 68 Jiyang Road, Suzhou, Jiangsu 215600, P.R. China
E-mail: 727570771@qq.com

Dr Qirong Dong, Department of Orthopedics, The Second Affiliated Hospital of Soochow University, 1055 Sanxiang Road, Suzhou, Jiangsu 215004, P.R. China
E-mail: dongqrvip@163.com

*Contributed equally

Abbreviations: LDI, low-dose ionizing radiation; PBS, phosphate-buffered saline; ROCK, Rho-associated protein kinase; TEM, transmission electron microscopy

Key words: osteoblasts, X-ray irradiation, cytoskeleton reorganization, RhoA/Rho-associated protein kinase

Introduction

X-rays are a type of ionizing radiation widely used in medicine, such as during imaging examinations and radiotherapy of malignant tumors (1). Previous studies have shown that high dose X-rays can lead to bone loss, which increases the risk of fractures (2,3) that do not heal easily (4,5).

Luckey previously proposed the theory of excitation effect of low dose X-ray irradiation (LDI), which has become a focus of interest over the years (6). Previous studies investigating bone tissue have revealed that LDI promotes osteoid matrix proliferation and mineralization (7,8). Furthermore, low dose X-rays are widely used in different branches of medicine, particularly in orthopedics (1). Patients with orthopedic diseases, including fracture and lumbar degenerative diseases often receive multiple doses of X-rays during therapy (9,10). Due to this, low dose X-rays have vital significance.

Previous research has shown that LDI could promote osteoblast proliferation and differentiation, whilst high dose X-rays can lead to bone loss (8,9,11,12). In a previous study, LDI promoted osteoblast differentiation and accelerated fracture healing in mice (12,13). Additionally, Park *et al* (7) demonstrated that doses of 1 and 2 Gy X-ray radiation significantly increased differentiation and mineralization of osteoblasts. However, the molecular mechanism by which LDI exerts its effects has not been elucidated. LDI may be associated with altered gene expression that is related to signal transduction, cell cycle regulation and cytoskeleton reorganization (14).

Microarrays demonstrated that LDI induced significant upregulation of LIM domain kinase 2 (LIMK2), and that this was associated with cytoskeleton reorganization (15-17). Furthermore, Kurpinski *et al* (18) reported that cytoskeleton and receptor signaling of human mesenchymal stem cells were uniquely activated in response to 0.1 Gy LDI.

The current study hypothesized that LDI may cause cytoskeleton rearrangement and affect cell morphology. Changes

in cytoskeleton reorganization may be the structural basis for the exchange of intracellular and extracellular information following LDI stimulation. The changes in adhesion signals may also affect biological processes, such as osteoblast proliferation and differentiation (19,20).

The cytoskeleton is mainly composed of actin microfilaments, which act as a mechanical support framework that maintains cell morphology, transduces various intracellular signals (21) and serves a crucial role in cell adhesion, motility, division and differentiation (22). Additionally, Ricci *et al* (23) reported that intact cytoskeletal actin filaments contribute to cell survival. The cytoskeleton is sensitive to extracellular stimuli, which can cause rapid reorganization of the actin cytoskeleton (23). Various stimuli, including fluid shear stress, magnetic field and ultrasound, regulate the actin cytoskeleton (24-27). The appropriate intensity of these stimuli may promote the reorganization of the cytoskeleton, thereby altering cell functions (24).

Nonetheless, few studies have addressed the effect of LDI on the osteoblast cytoskeleton. Onoda *et al* (28) demonstrated that LDI induced the reorganization of fiber (F) actin microfilaments of pulmonary microvascular endothelial cells. However, 24 h post-irradiation, the depolymerized microfilaments reverted to their pre-irradiation states. These results indicated that various complex pathways may regulate the process of actin reorganization.

Small GTPases of the Rho family have been researched extensively. RhoA and its effectors serve a crucial role in regulating cytoskeleton arrangement and various essential cellular processes, including proliferation and differentiation (29,30). RhoA is the prototypical member of the Rho family and responds to plasma membrane receptors for various stimuli, including cytokines and environmental stress (31). Furthermore, RhoA controls stress-mediated fiber formation by regulating certain downstream key proteins (31,32). The most extensively studied RhoA effector protein is Rho-associated kinase (ROCK) 1, which mediates actin contractility by phosphorylating myosin light chains (31,32). Moreover, ROCK proteins may phosphorylate and activate LIMKs, which phosphorylate cofilin (31,32). Cofilin is involved in the reorganization of the actin cytoskeleton (33).

The present study investigated the effects of X-ray irradiation on the morphology and cytoskeleton of MC3T3-E1 cells. Additionally, the roles of the RhoA/ROCK pathway in this process were investigated to determine the biological effects of LDI.

Materials and methods

Cell culture. Pre-osteoblastic MC3T3-E1 cells were obtained from the Institute of Biochemistry and Cell Biology. A total of $1x10^5$ cells were cultured in α-MEM supplemented with 10% FBS, 5 mM β-glycerophosphate, 50 μg/ml ascorbic acid and 100 nM dexamethasone (all Sigma-Aldrich; Merck KGaA) at 37˚C with 5% CO_2. Fresh medium was replaced every three days and cells were sub-cultured at 80% confluency.

Irradiation of osteoblastic cells. A total of $2x10^4$ MC3T3-E1 cells were exposed to 0 (control), 0.5 or 5 Gy X-ray irradiation (at a rate of 200 cGy/min) emitted by a medical linear accelerator (Siemens Primus) at room temperature using a 6 MV radiation source. The time at irradiation was defined day 0.

Transmission electron microscopy (TEM). MC3T3-E1 cells were cultured for 3 days, fixed in 2.5% glutaraldehyde for 2 h at 4˚C and rinsed three times (15 min each time) with 0.1 M sodium phosphate buffered saline (PBS). Post-fixation was then performed with 1% osmium tetroxide (Beyotime Institute of Biotechnology) for 3 h at room temperature. Subsequently, the cells were dehydrated through an ascending gradient of ethanol and immersed in acetone. Samples were then embedded and double stained in 2% aqueous uranyl acetate and Satoh's lead citrate at 4˚C for 2 h, and observed with a transmission electron microscope (magnification, x5,000; JEM-1200EX; JEOL, Ltd.) operated at 85 kV.

Labeling of F-actin cytoskeleton for fluorescence microscopy. MC3T3-E1 cells were seeded ($1.0x10^4$ cells/ml) on poly-L-lysine-coated glass coverslips in 24-well plates and cultured in an osteogenic differentiation medium (containing 50 μg/ml ascorbic acid and 10 mM β-glycerophosphate; Beyotime Institute of Biotechnology). Following X-ray irradiation, cells were gently washed with PBS at 37˚C at time points 2 h, 1, 3 or 5 days post-irradiation. Cells were then fixed with 4% paraformaldehyde (pH 7.4) for 20 min at room temperature and permeabilized with 0.1% Triton X-100 for 5 min at room temperature. Cells were then washed three times with PBS and blocked with 1% bovine serum albumin (Beyotime Institute of Biotechnology) for 30 min at room temperature and incubated with FITC-conjugated phalloidin (Sigma-Aldrich; Merck KGaA; 1:100) in the dark for 1 h at room temperature. Cell nuclei were stained with 100 nM DAPI for 10 min at room temperature, followed by analysis using a fluorescence microscope (magnification, x200).

Actin is the main component of the cytoskeleton (21). FITC-conjugated phalloidin is a specific dye for F-actin and glows green after binding to polymerized F-actin (23). F-actin expression can be quantitatively analyzed according to the intensity of green fluorescence in cells. Therefore, the mean fluorescence intensity of each group of cells was calculated to compare the content of actin in each group.

ImageJ software (version 1.8.0; National Institutes of Health) was used to randomly analyze the images of six cells with clear boundaries within the slide and the average fluorescence intensity of each cell (average fluorescence intensity=fluorescence intensity/cell area) was measured as the analysis index. Data are presented as the mean ± standard deviation, and represented the mean fluorescence intensity. 'Area' represents the total area of cells counted, 'Min' represents the lowest fluorescence intensity and 'IntDen' represents the total fluorescence intensity.

Total RNA extraction and gene expression analysis by reverse transcription-quantitative PCR (RT-qPCR). MC3T3-E1 cells were cultured in osteogenic differentiation medium following X-ray irradiation. The cells were harvested on days 3 and 7 after irradiation. Total RNA was extracted using TRIzol® (Invitrogen, Thermo Fisher Scientific, Inc.), according to the manufacturer's protocol. cDNA was obtained from total

RNA (1 μg) using RevertAid First Strand cDNA Synthesis kit (cat. no. K1622; Fermentas; Thermo Fisher Scientific, Inc.). The reaction system was incubated at 42˚C for 1 h, and treated at 70˚C for 10 min. The first cDNA strand was obtained and stored at -20˚C. qPCR was performed in a total volume of 20 μl, which consisted of 1 μl cDNA (500 ng), 1 μl gene-specific 10 μM PCR primer-pair stock and 10 μl SsoFast™ EvaGreen® Mix (Bio-Rad Laboratories, Inc.) using the Bio-Rad CFX96 system according to the manufacturer's protocol. The expression of RhoA, ROCK1, LIMK2 and β-actin was detected by RT-PCR. The specific primers used are listed in Table I. The thermocycling conditions consisted of initial denaturation at 95˚C for 30 sec, followed by 40 cycles of 5 sec at 95˚C and 5 sec at 60˚C, which were subsequently followed by the melting curve test. The relative mRNA expression normalized to β-actin was expressed as a fold change, which was calculated using the comparative Ct ($2^{-\Delta\Delta Cq}$) method (34) using the control group as a reference with $2^{-\Delta\Delta Cq}$=1.

Protein extraction and immunoblotting. A total of $1x10^6$ MC3T3-E1 cells were lysed on ice with RIPA lysis buffer (Beyotime Institute of Biotechnology) containing protease and phosphatase inhibitors (Beyotime Institute of Biotechnology) after being cultured for 1, 3 or 5 days. The supernatant was collected by centrifugation at 12,000 x g for 15 min at 4˚C, and the protein concentration was quantified using a bicinchoninic acid assay (Beyotime Institute of Biotechnology). Protein samples (30 μg/lane) were resolved using 10% SDS-PAGE and transferred onto PVDF membranes (EMD Millipore). Membranes were blocked with 5% non-fat dried milk in Tris-buffered saline with 0.1% Tween 20 (TBST) for 2 h at room temperature. Membranes were incubated overnight at 4˚C with the following antibodies: Rabbit anti-cofilin (cat. no. 3312; dilution 1:1,000; Cell Signaling Technology, Inc.), rabbit anti-ROCK1 (cat. no. 4035; dilution 1:2,000; Cell Signaling Technology, Inc.), rabbit anti-phospho-LIMK2 (cat. no. 3845; dilution 1:2,000; Cell Signaling Technology, Inc.), rabbit anti-phospho-cofilin (cat. no. 3311; dilution 1:2,000; Cell Signaling Technology, Inc.) and β-actin (cat. no. 4967; dilution 1:3,000; Cell Signaling Technology, Inc.). Following three washes with TBST, membranes were incubated with horseradish peroxidase-conjugated anti-rabbit IgG secondary antibody (cat. no. ab97200; dilution 1:2,000; Abcam) for 1 h at room temperature. Immunoreactive bands were visualized using enhanced chemiluminescence detection reagents (ECL; EMD Millipore) and images were captured using a chemiluminescence imaging system (Kodak). Densitometric analysis was performed using the ImageJ software (version 1.8.0; National Institutes of Health).

RhoA activation assay. A total of $1x10^6$ MC3T3-E1 cells were harvested on days 1, 3 and 5 following X-ray irradiation and lysed with RIPA buffer (Beyotime Institute of Biotechnology) buffer. the protein concentration was determined using a bicinchoninic acid protein assay kit (Beyotime Institute of Biotechnology). A total of 30 μl the supernatant was used to determine the expression of total RhoA. The remaining supernatant was used to isolate GTP-bound RhoA using an Active GTPase Pull-down kit (cat. no. 16116; Thermo Fisher Scientific, Inc.), which used the glutathione S-transferase-Rhotekin Rho binding domain (EMD Millipore), according to the manufacturer's protocol. The eluted proteins were then separated using 15% SDS-PAGE, transferred to PVDF membranes (EMD Millipore). After blocking with 5% skim milk in TBST for 2 h at room temperature, the membranes were incubated overnight with specific anti-RhoA antibodies (1:100; cat. no. sc-418; Santa Cruz Biotechnology, Inc.). Total RhoA protein was detected via western blotting. Immunoreactive bands were visualized using ECL (EMD Millipore) and band intensity was quantified using ImageJ v1.8.0 software.

Y-27632 inhibition of ROCK1. MC3T3-E1 cells were pretreated with 10 μmol/l Y-27632 (EMD Millipore) at 37˚C for 30 min prior to X-ray irradiation. After being cultured for 1, 3 or 5 days, cells in each group were labeled with FITC-phalloidin to observe the changes in the cytoskeleton using the protocols aforementioned. The fluorescence intensity of the cells was quantitatively analyzed using ImageJ v1.8.0 software.

Alkaline phosphatase staining. MC3T3-E1 cells were cultured in 24-well plates at a density of $1x10^4$ cells/well. Cells were then treated with the 0, 0.5 and 5 Gy X-ray doses. The medium was discarded on day 7. Alkaline phosphatase staining was carried out using the Alkaline Phosphatase Assay Kit (cat. no. P0321, Beyotime Institute of Biotechnology) at room temperature for 30 min according to the manufacturer's protocol and observed using an inverted light microscope (magnification, x10).

Alizarin red staining. MC3T3-E1 cells were cultured in 24-well plates at a density of $1x10^4$ cells/well and treated with 0, 0.5 and 5 Gy X-ray. The medium was changed once every 3 days and discarded on day 12. After washing with PBS, cells were fixed with 4% paraformaldehyde at room temperature for 20 min and were stained with 1% alizarin red dye (pH 4.2) at room temperature for 30 min. Mineralized nodules were visualized using a light microscope (magnification, x20).

Statistical analysis. Data are presented as mean ± SD and all experiments were performed in triplicate. Differences between the groups were analyzed by one-way ANOVA followed by Student-Newman-Keuls test using SPSS software (version 18.0; SPSS, Inc.). $P<0.05$ was considered to indicate a statistically significant difference.

Results

Effects of irradiation on MC3T3-E1 cell morphology. MC3T3-E1 cells cultured in α-MEM supplemented with 10% FBS adhered and formed cell colonies with irregular morphology, mainly exhibiting fusiform shape, and had large nuclei and observable nucleoli. After 3 days, the cells aggregated in a semi-confluent state, cell number increased and cell bodies were markedly enlarged. After 5 days, the cells formed confluent monolayers.

The unirradiated cells proliferated and exhibited small cell volumes, plump cell bodies and abundant cytoplasm, with cells in the dividing phase exhibiting irregular shapes (Fig. 1A). No notable difference was detected between the 0.5 Gy group and the control group (Fig. 1B). The 5 Gy group exhibited decreased cell numbers, enlarged cell bodies, homogenous

Table I. Primer sequences used for reverse transcription-quantitative PCR.

Gene	Forward primer sequence (5'-3')	Reverse primer sequence (3'-5')	Amplification length (bp)
β-actin	GAGACCTTCAACACCCCAGC	CCACAGGATTCCATACCCAA	446
RhoA	CGCTTTTGGGTACATGGAGT	GTGGGCTCAGTCAAAAGCTC	79
LIMK2	GTGGGCTCAGTCAAAAGCTC	CCACAAGGGTGCAAAGAAAT	284
ROCK1	AGGCGGTGATGGCTATTATG	CCCAACCAAAGAATCTGCAT	190

LIMK2, LIM domain kinase 2; ROCK1, Rho-associated protein kinase 1.

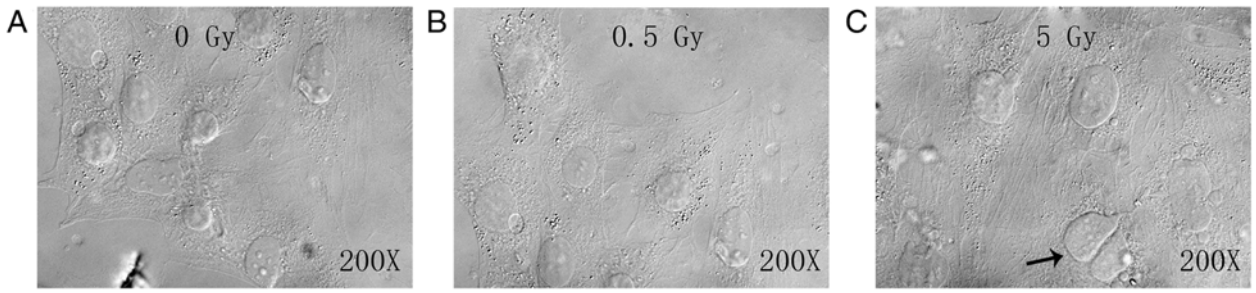

Figure 1. Effects of irradiation on MC3T3 cell morphology. (A) Cells in the unirradiated group had small cell volumes, plump cell bodies and abundant cytoplasm. (B) Cell morphology in the 0.5 Gy group was similar to that of the unirradiated group. (C) The 5 Gy group exhibited increased cell volumes, and multinucleated giant cells and black particles were observed in the cytoplasm. Arrow indicates multinucleated giant cells. Magnification, x200.

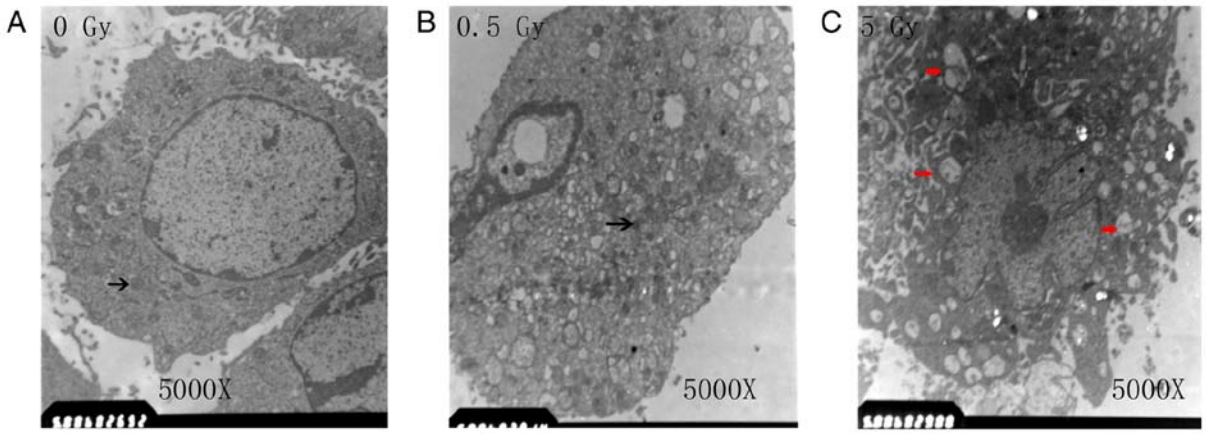

Figure 2. Changes in intracellular microstructure of MC3T3 cells following X-ray irradiation. (A) The 0 Gy group exhibited abundant intracellular organelles and observable nuclei. Observation of golgi bodies and endoplasmic reticulum was common, while that of lysosomes was scarce. (B) The intracellular microstructure of the 0.5 Gy group was similar to that of the 0 Gy group, with an increased number of organelles. (C) The number of organelles decreased in the 5 Gy group, while the number of lysosomes increased. Black arrow indicates endoplasmic reticulum. Red arrows indicate enlarged vacuoles and nuclear lysis. Magnification, x5,000.

cytoplasm and reduced refraction. Additionally, numerous black particles and vacuoles were observed in the cytoplasm, along with multinucleated giant cells (as indicated by arrow; Fig. 1C).

Observation of microstructural changes by TEM. Cells in the control and the 0.5 Gy groups exhibited abundant intracellular organelles and had observable nuclei. Additionally, observation of intracellular Golgi bodies and endoplasmic reticulum was common, while that of lysosomes was rare (Fig. 2A and B). In the 5 Gy group, the nuclear chromatin was condensed, the number of organelles decreased and the number of enlarged vacuoles was increased (as indicated by the red arrows; Fig. 2C).

F-actin staining. At 2 h post-irradiation, cells in the 0.5 and 5 Gy groups exhibited decreased size and F-actin fluorescence intensity compared with controls (Fig. 3). Furthermore, the formation of stress fibers decreased and their arrangement was sparse, disorganized, discontinuous or broken. Additionally, the amount of crystallized actin increased in the treated cells, particularly in the 5 Gy group. After 1 day, F-actin began to

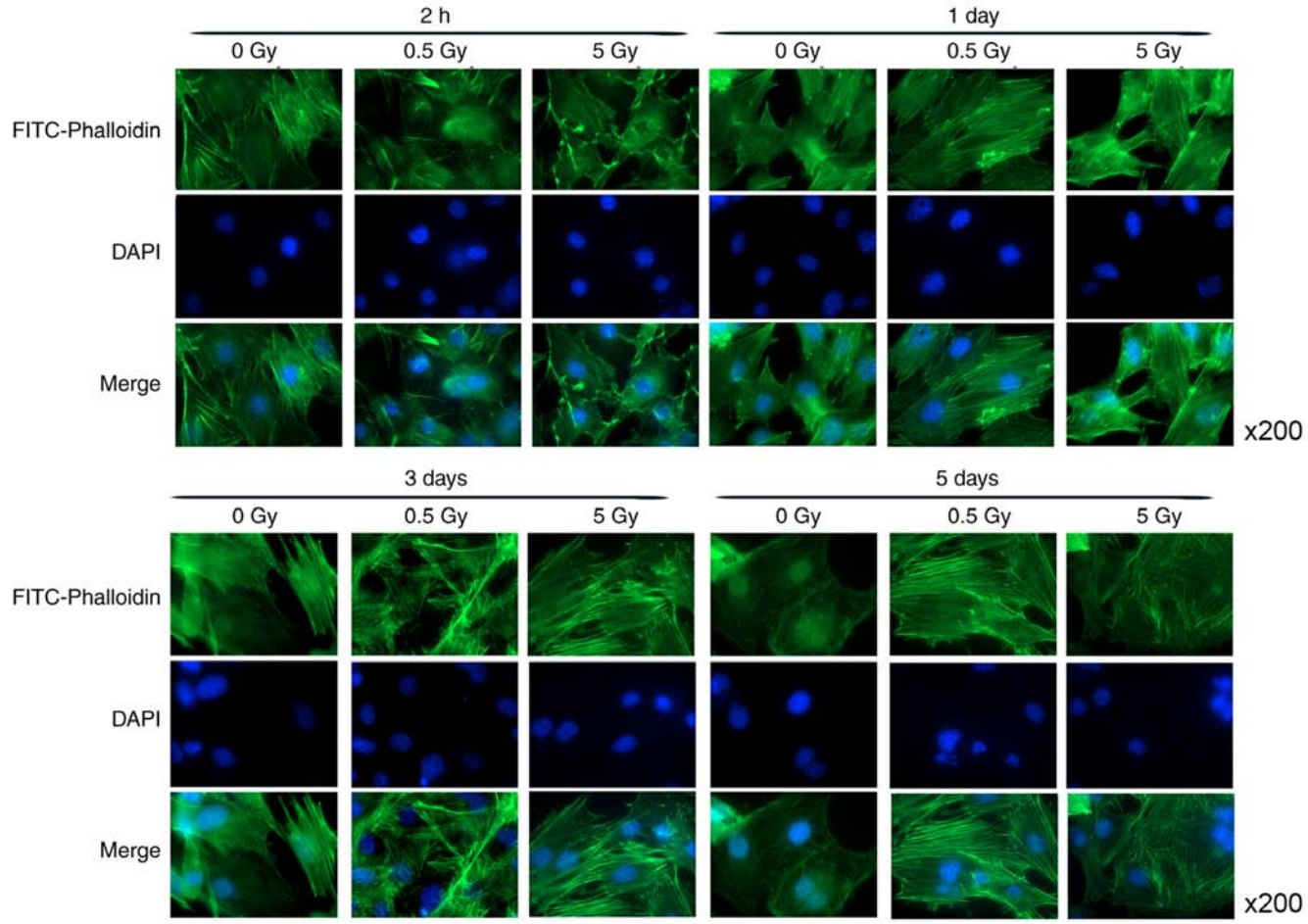

Figure 3. Low dose X-ray radiation-induced reorganization of the actin cytoskeleton was visualized using F-actin staining in MC3T3 cells. Cells were irradiated for 24 h with 0, 0.5 or 5 Gy X-rays. Cells were then fixed and fluorescence-labeled with FITC-phalloidin and stained with DAPI. Magnification, x200.

thicken and rearranged in the 0.5 Gy group and fluorescence intensity was significantly increased compared with controls (Fig. 4). At 3 days post-irradiation, fluorescence intensity in the 0.5 Gy group was significantly increased compared with that in the 0 and 5 Gy groups (Fig. 4). By day 5, F-actin fluorescence intensity in the 0.5 Gy group returned to normal (Fig. 4).

ImageJ software was used to randomly analyze the images of six cells with clear boundaries within the slide and the average fluorescence intensity of each cell (average fluorescence intensity=fluorescence intensity/cell area) was measured as the analysis index (Table II).

The results demonstrated that fluorescence intensity of the 0.5 and 5 Gy groups were significantly decreased compared with controls following 2 h of X-ray irradiation ($P<0.05$; Fig. 4). At 24 h post-irradiation, intensity in the 0.5 Gy group was significantly increased compared with controls and the 5 Gy group ($P<0.05$; Fig. 4). The fluorescence intensity in the 5 Gy group was not significantly increased compared with controls ($P>0.05$; Fig. 4). Following 3 days irradiation, the intensity in the 0.5 Gy group reached a peak value that was significantly increased compared with the other two groups ($P<0.05$; Fig. 4). Additionally, the intensity in the 5 Gy group increased, but not significantly compared with controls. At 5 days post-irradiation, the fluorescence intensity of the 0.5 and 5 Gy groups decreased, but not significantly when compared with controls (Fig. 4).

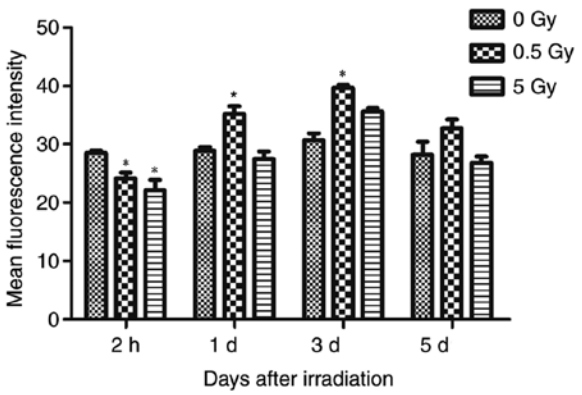

Figure 4. Comparison of average fluorescence intensity of F-actin staining in 0, 0.5 and 5 Gy groups group. The values were presented in bar graphs as mean ± SD of average fluorescence intensity. *$P<0.05$ vs. 0 Gy.

Effects of irradiation on RhoA, ROCK1 and LIMK2 expression. Previous studies have revealed that LIMK1 and LIMK2 are activated by Rho GTPases (26,29,35). These molecules induce cytoskeleton reorganization by phosphorylating and inactivating the actin depolymerization of cofilin (35). The expression of genes associated with the formation of actin filaments, including RhoA, ROCK1 and LIMK2, were examined using RT-qPCR on days 3 and 5 days following

Table II. Fluorescence intensity of fiber actin in MC3T3-E1 cells following X-ray irradiation.

A, 2 h post-irradiation

Radiation dose (Gy)	Area	Mean ± SD	Min	IntDen	P-value[a]
0	256,956	29.107±13.296	15	7,479,102	/
0.5	250,396	25.329±12.209	12	6,342,378	0.045
5	248,358	27.021±13.049	12	6,710,960	0.036

B, 1 day post-irradiation

Radiation dose (Gy)	Area	Mean ± SD	Min	IntDen	P-value
0	213,267	30.865±14.266	22	8,075,451	/
0.5	270,394	37.176±16.750	16	10,052,197	0.038
5	200,453	36.728±15.782	12	7,362,259	0.525

C, 3 days post-irradiation

Radiation dose (Gy)	Area	Mean ± SD	Min	IntDen	P-value
0	264,269	35.645±17.213	10	9,419,783	/
0.5	253,611	38.687±18.072	15	9,811,449	0.047
5	285,670	36.039±12.128	12	10,295261	0.325

D, 5 days post-irradiation

Radiation dose (Gy)	Area	Mean ± SD	Min	IntDen	P-value
0	198,053	27.309±15.039	13	5,408,629	/
0.5	275,760	28.527±14.107	18	7,866,606	0.416
5	251,803	27.258±13.322	9	6,863,646	0.512

[a]vs. 0 Gy group. Area, total area of cells counted; SD, standard deviation; Min, lowest fluorescence intensity; IntDen, total fluorescence intensity.

irradiation. The results demonstrated that RhoA, ROCK1 and LIMK2 expression was significantly upregulated following irradiation with 0.5 Gy compared with those irradiated with 0 Gy ($P<0.05$; Fig. 5A-C).

At 3 and 5 days post-irradiation, the expression of RhoA in the 0.5 Gy group was significantly higher than that in the control and 5 Gy groups ($P<0.05$; Fig. 5A). Additionally, RhoA was significantly higher in the 5 Gy group compared controls 3 days post-irradiation; however, no significant difference was detected on day 5 ($P>0.05$; Fig. 5A). LIMK2 expression in the 0.5 and 5 Gy groups was significantly higher compared with controls at 3 and 5 days post-irradiation ($P<0.05$; Fig. 5C), but no significant difference was detected between the two groups (Fig. 5C). ROCK1 expression in the 0.5 Gy group was significantly higher compared with the control and 5 Gy groups at days 3 and 5 ($P<0.05$), but no significant difference was detected between the 5 and 0 Gy groups (Fig. 5B).

Synthesis of cytoskeletal proteins. RhoA, ROCK1, LIMK2, phosphorylated LIMK2 (p-LIMK2), cofilin and phosphorylated cofilin (P-cofilin) protein expression was assessed by western blotting (Figs. 6-9) and RhoA, ROCK1, LIMK2, phosphorylated LIMK2 (p-LIMK2) demonstrated similar expression levels when compared with mRNA expression. The expression levels of cofilin and phosphorylated cofilin (p-cofilin) were consistent with other cytoskeletal related proteins.

RhoA activation via GTP-loading in X-ray-irradiated osteoblasts was analyzed to determine the significance of RhoA in radiation response. A low level of GTP-RhoA was detected in non-irradiated (0 Gy) cells (Fig. 7A). This level increased significantly at 1 day post-irradiation in the 0.5 Gy group compared with controls and the 5 Gy group (Fig. 7A), indicating that RhoA was rapidly activated in osteoblasts. This increase was most pronounced on day 3 in the 0.5 Gy group compared with controls and the 5 Gy group (Fig. 7A). No significant difference was observed in the total RhoA level between groups (Fig. 7B). The variation trend of active-RhoA/RhoA ratio in each group was similar to that of active-RhoA (Fig. 7C). Furthermore, P-LIMK2 expression significantly increased on days 3 and 5 following

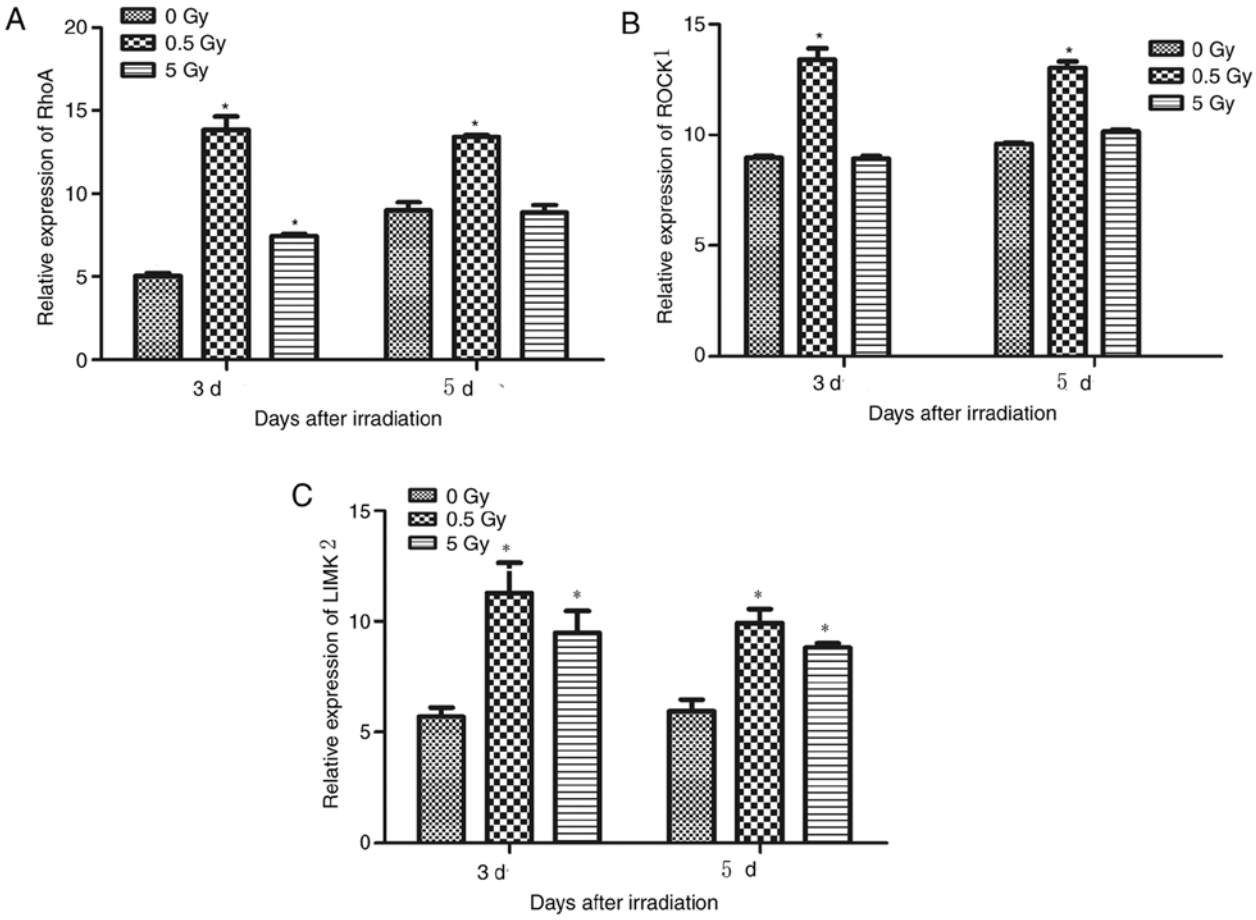

Figure 5. Relative (A) RhoA, (B) ROCK1, and (C) LIMK2 mRNA expression in irradiated MC3T3-E1 cells in response to different doses of X-ray irradiation. *P<0.05 vs. 0 Gy. ROCK1, Rho associated kinase 1; LIMK2, LIM domain kinase 2.

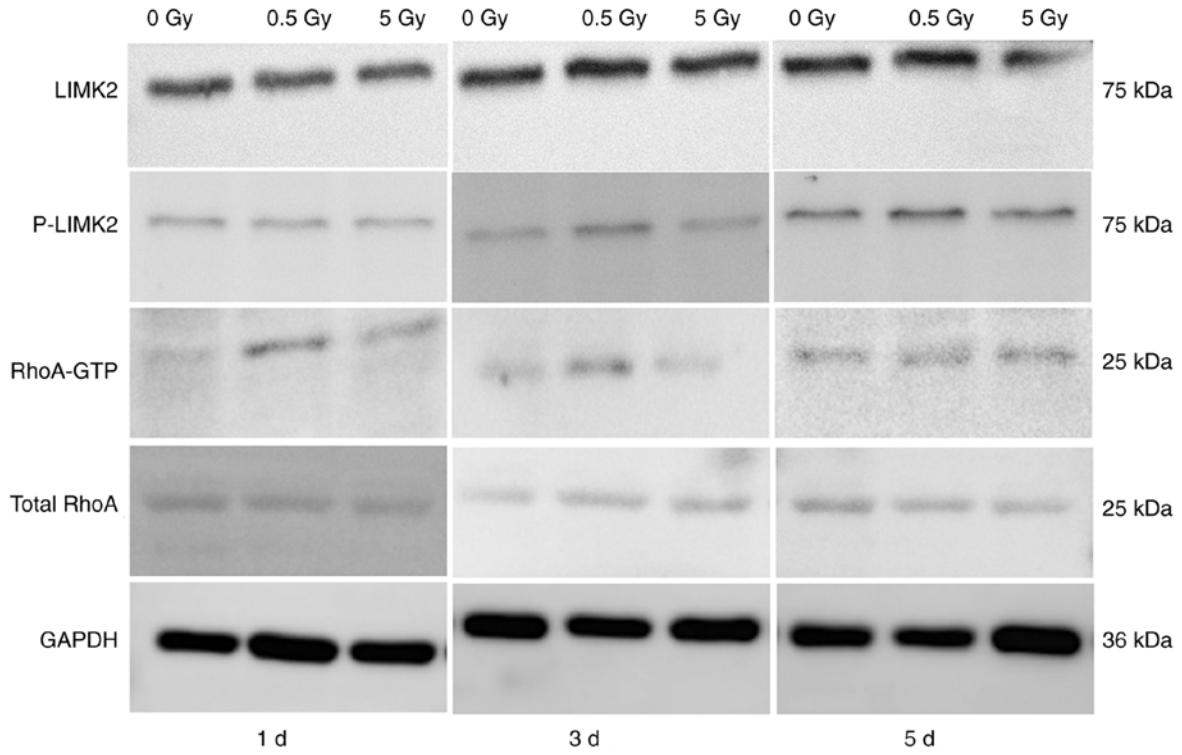

Figure 6. Low dose X-ray irradiation-induced rapid GTP loading of RhoA and LIMK2 phosphorylation. Active GTP-bound RhoA expression was determined using a glutathione S-transferase pull-down assay. Expression of active RhoA, total RhoA, P-LIMK2 and LIMK2 in MC3T3-E1 cells following X-ray irradiation were visualized via western blotting. LIMK2, LIM domain kinase 2; P-LIMK2, phosphorylated LIM domain kinase 2.

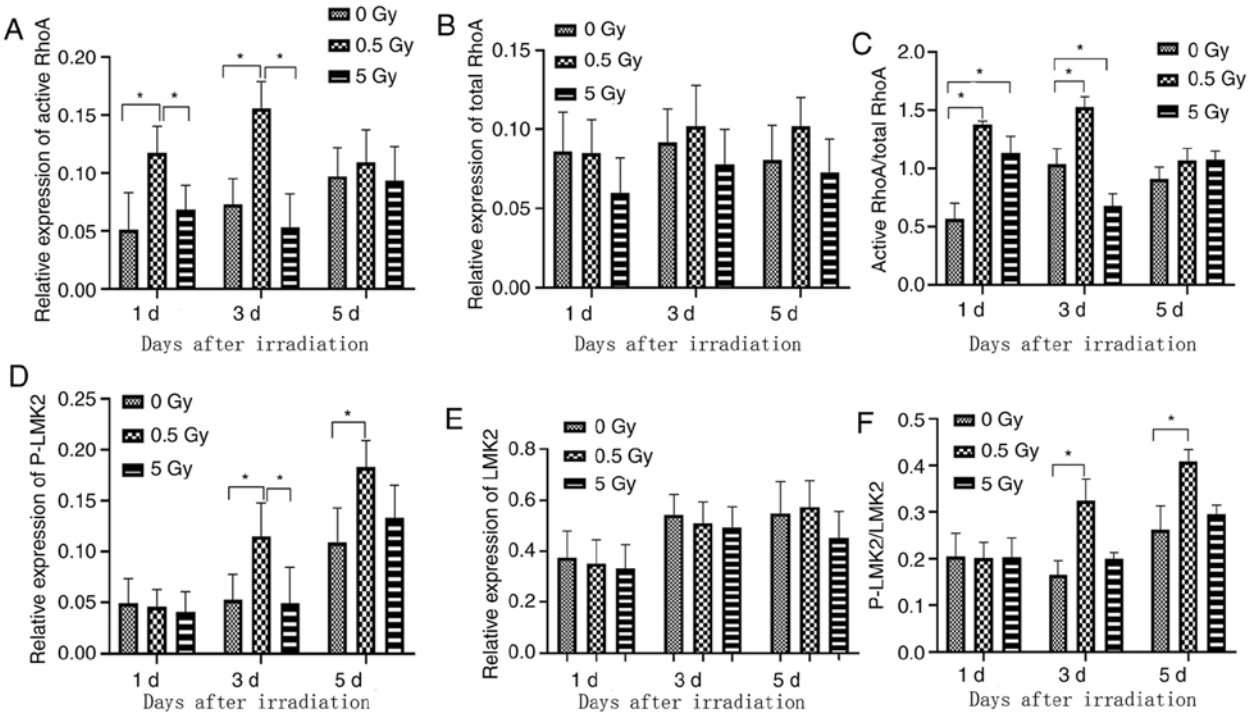

Figure 7. The immunoblots of (A) active RhoA, (B) total RhoA, (C) normalized Rho GTP, (D) P-LIMK2, (E) LIMK2 and (F) normalized P-LIMK were analyzed using densitometry. The results are presented in bar graphs as mean ± S.D. *P<0.05. P-LIMK2, phosphorylated LIM domain kinase 2; LIMK2, LIM domain kinase 2.

0.5 Gy irradiation compared with controls and 5 Gy groups (Fig. 7D). No significant difference was observed in the total LIMK2 level between groups (Fig. 7E). The variation trend of p-LIMK2/LIMK2 ratio in each group was similar to that of p-LIMK2 (Fig. 7F). These results indicated that RhoA was a critical downstream regulator of X-ray irradiation-induced actin reorganization.

At 1 day post-irradiation, ROCK1 expression in the 0.5 Gy group was significantly increased compared with the control group. On day 3, ROCK1 expression was also significantly increased compared with controls (P<0.05, Fig. 9C) and reached a peak value at day 5 (P<0.05, Fig. 9C). Furthermore, P-cofilin level was higher 1 day post-irradiation in the 0.5 Gy group compared to the control and 5 Gy groups, but this difference was not statistically significant (Fig. 9A). However, there was a statistically significant increase in expression on days 3 and 5 post-irradiation in the 0.5 Gy group compared with the control groups (P<0.05; Fig. 9A). Additionally, P-cofilin expression was significantly higher in the 5 Gy group compared with controls on days 3 and 5 (Fig. 9A). Furthermore, cofilin expression was not significantly different between groups on days 1 and 3 post-irradiation; however, on day 5 expression was significantly increased in the 0.5 Gy group compared with control and 5 Gy groups (P<0.05; Fig. 9B). The expression of P-cofilin/cofilin was significantly higher in the controls compared with the 0.5 and 5 Gy groups on day 1 (P<0.05; Fig. 9D). However, P-cofilin/cofilin expression was significantly increased in the 0.5 and 5 Gy groups compared with controls on day 3, and between the 0.5 group and controls on day 5 (P<0.05; Fig. 9D). No significant difference was detected between the 0.5 and 5 Gy groups on all timepoints tested (Fig. 9D).

F-actin staining in cells pretreated with ROCK1 inhibitor Y-27632 (10 µmol/l) for 30 min prior to X-ray irradiation. The results demonstrated green fluorescence in all cells 1 day following X-ray irradiation and Y-27632 pretreatment (Table III, Fig. 10A-C). However, fluorescence intensity was significantly weaker in the 0 Gy group compared with other groups after 1 day. Deformed tension fibers and unorganized thin filaments were observed (Fig. 10A). The fluorescence intensity of all groups was increased on day 3 compared with the intensity on day 1 (Fig. 5B). This intensity was further increased on day 5 and the tension fibers were organized and had returned to baseline (Fig. 10C).

At 1 day post-irradiation and -Y-27632 treatment, no significant difference was detected in the fluorescence intensity between the 0.5 and 5 Gy groups and controls (Fig. 10D). However, 3 days post-irradiation and -treatment, the fluorescence intensity and the number of tension fibers of all groups increased. Additionally, the fluorescence intensity of cells in the 0.5 Gy group was significantly increased compared with the control and 5 Gy groups (P<0.05; Fig. 10D). By day 5, the tension fibers were arranged into stress fibers, F-actin gradually returned to baseline and no significant difference was detected in fluorescence intensity among the groups (P>0.05; Fig. 10D).

Identification of osteoblasts. Following alkaline phosphatase staining, the cytoplasm of osteoblasts with purple granules, indicating staining was positive for alkaline phosphatase expression on the cell membrane surface of the osteoblasts (Fig. 11). Alkaline phosphatase serves as a marker enzyme for the differentiation and maturation of osteoblast, indicating the various stages of osteoblast differentiation (36).

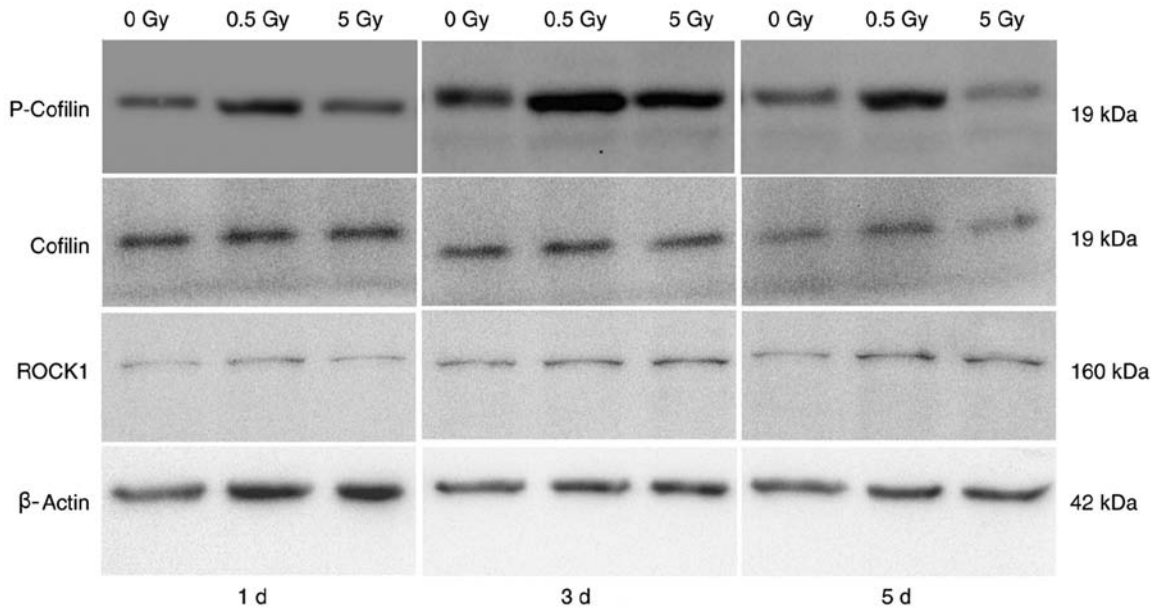

Figure 8. Western blotting of ROCK1, cofilin and P-cofilin in MC3T3-E1 cells following X-ray irradiation. ROCK1, Rho associated kinase 1; P-cofilin, phosphorylated cofilin.

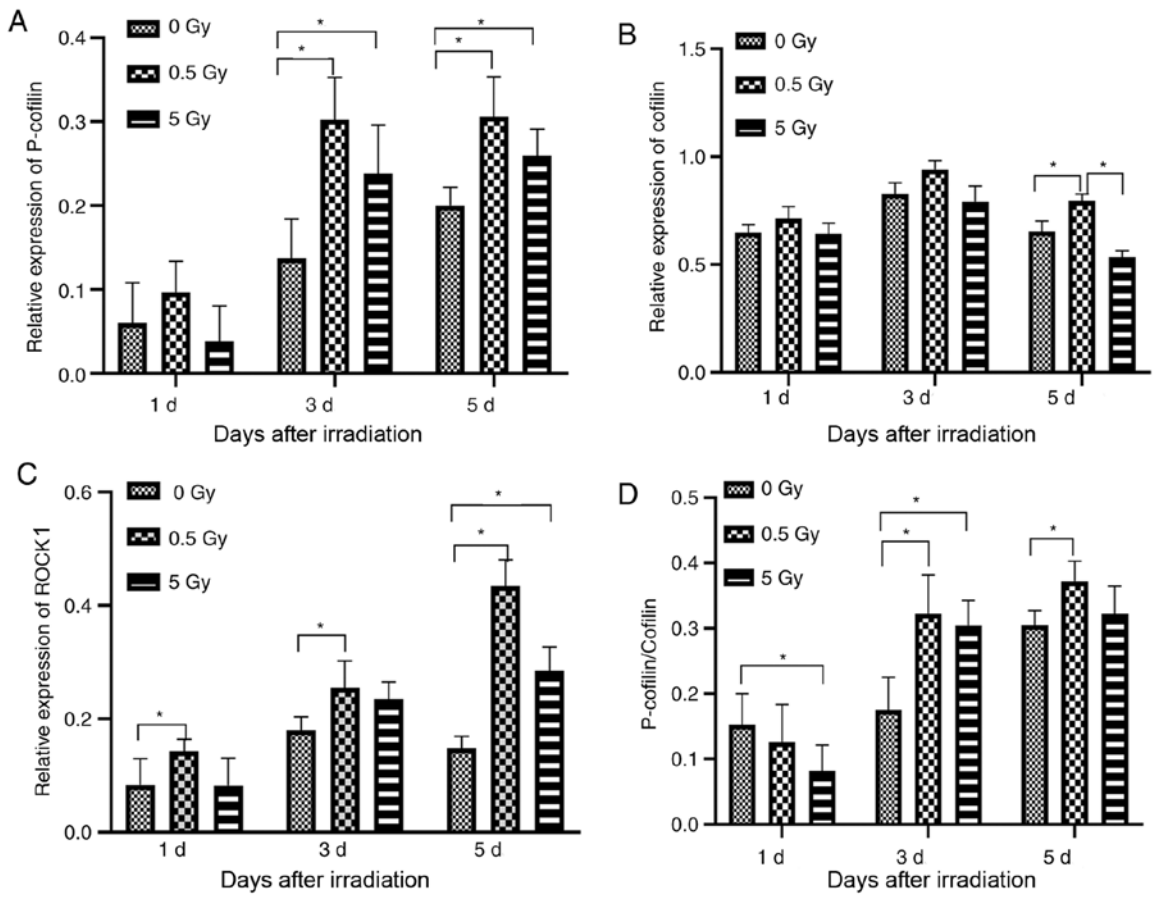

Figure 9. Low dose X-ray irradiation promoted ROCK1 and P-cofilin expression in MC3T3 cells. (A) P-cofilin, (B) cofilin, (C) ROCK1 normalized to β-actin and (D) normalized P-cofilin. *P<0.05.

Following 21 days in culture, the osteoblasts converged and showed multiple layers of overlapping growth. Their cell arrangement centered on mineralized nodules. Following alizarin red staining, multiple orange mineralized nodules of various sizes were observed (Fig. 12). Mineralization is a critical biological characteristic of osteoblasts (36). The results showed a satisfactory mineralization function of the cultured osteoblasts.

Table III. Fluorescence intensity of Y-27632-pretreated MC3T3-E1 cells in each group.

A, 1 day post-irradiation

Radiation dose (Gy)	Area	Mean ± SD	Min	IntDen
0	277,623	22.035±11.503	13	6,117,423
0.5	272,308	23.513±11.986	15	6,402,778
5	190,825	22.761±17.157	13	4,343,367

B, 3 days post-irradiation

Radiation dose (Gy)	Area	Mean ± SD	Min	IntDen
0	252,417	26.306±15.477	7	6,640,082
0.5	232,329	31.277±11.777	15	7,266,554
5	260,815	26.502±13.742	13	6,912,119

C, 5 days post-irradiation

Radiation dose (Gy)	Area	Mean ± SD	Min	IntDen
0	238,070	30.361±16.946	10	7,227,973
0.5	284,840	32.241±14.872	13	9,183,526
5	284,334	30.307±16.136	3	8,617,311

Area, total area of the cells counted; SD, standard deviation; Min, lowest fluorescence intensity; IntDen, total fluorescence intensity.

Discussion

The cytoskeleton is dynamic network of interconnected polymers that regulates the mechanical properties of cells and maintains cell morphology, cell division and intracellular transportation (37,38). Additionally, the cytoskeleton is closely associated with cell migration, phagocytosis, pinocytosis and secretion (39,40) and serves a major role in transducing a variety of intracellular signals (41). Therefore, changes in the cytoskeleton inevitably affect cell function.

The cytoskeleton mainly consists of microtubules, microfilaments and intermediate filaments (21). Microfilaments are mainly composed of actin in the form of free globular (G-) or F-actin (21). Mechanical stimulation causes intracellular free G-actin aggregation, resulting in the formation of F-actin (26). Microfilaments serve a role in maintaining cell morphology, tight intercellular connections and extracellular matrix adhesion and are sensitive to ionizing radiation (42). The dynamics of actin polymerization and depolymerization regulate cell movement, adhesion and the cell division cycle (43). Ionizing radiation can damage the membrane cytoskeleton, which affects cellular function (43).

In the current study, X-ray irradiation caused intracellular morphological and microstructural changes in osteoblasts. Cells irradiated by 0 and 0.5 Gy X-rays exhibited abundant intracellular organelles, such as Golgi bodies and endoplasmic reticulum, which are related to the enhancement of cell proliferation and differentiation (13). However, in cells irradiated with 5 Gy X-rays, the nuclear chromatin condensed, the number of lysosomes increased and the number of intracellular organelles decreased. Additionally, various necrosis-related changes, including enlarged vacuoles and homogeneous nuclear lysis, were observed. These results were hypothesized to be related to direct cellular damage caused by high doses of radiation.

A previous *in vitro* study demonstrated that ionizing radiation can damage cellular actin networks and endothelial cell barrier function (28). Human respiratory epithelial cell line alu3 and 16HBEl40 were treated with 2-10 Gy irradiation and the results demonstrated that F-actin was significantly reduced and intracellular crystallized actin expression was increased. These results indicated that radiation caused an increase in F-actin depolymerization (44). Furthermore, these cytoskeleton changes affected the connections between cells, resulting in increased permeability and the formation of cell gaps (44).

In the current study, unirradiated cells exhibited normal cell morphology and F-actin was organized. At 2 h post-irradiation, unirradiated cells shrank and became plump. Subsequently, F-actin depolymerized and its fluorescence intensity decreased, which indicated a disorganized and discontinuous state, particularly in the 5 Gy group. The cause of these changes was attributed to ionizing radiation, which lead to cytoskeleton damage, fracture and collapse. However, the 0.5 Gy group exhibited different changes. At 2 h post-irradiation, the arrangement of microfilaments was disordered and discontinuous, similar to that of the 5 Gy group. However, intracellular actin became thick and rearranged 24 h post-irradiation. As a result, the fluorescence intensity increased, indicating that F-actin expression was significantly increased following LDI.

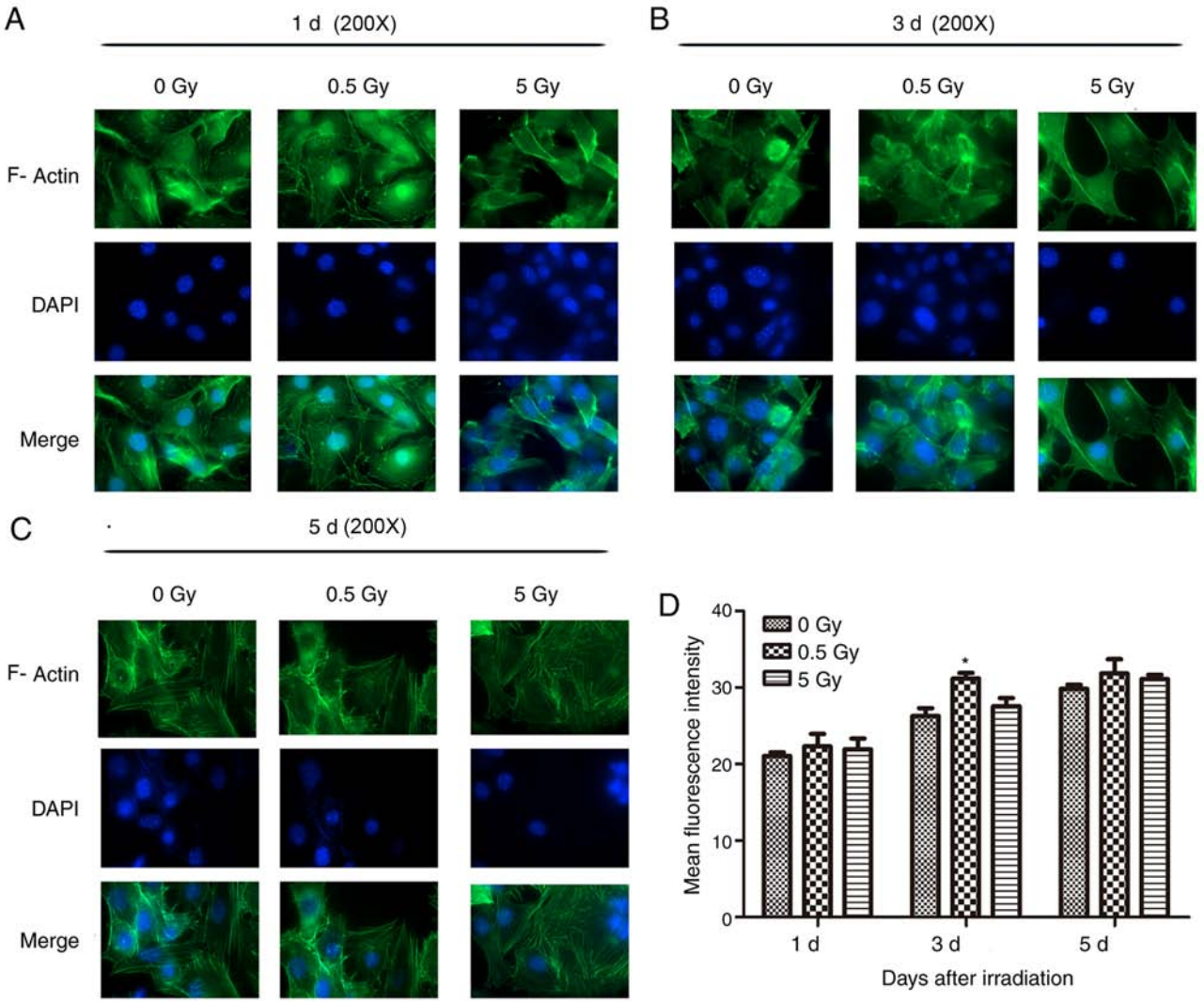

Figure 10. ROCK1 inhibitor Y-27632 pretreatment and F-actin staining in MC3T3 cells. F-actin staining of cells on post-irradiation on days (A) 1, (B) 3 and (C) 5. (D) Y-27632 partially inhibited LDI-mediated actin reorganization. Magnification, x200.

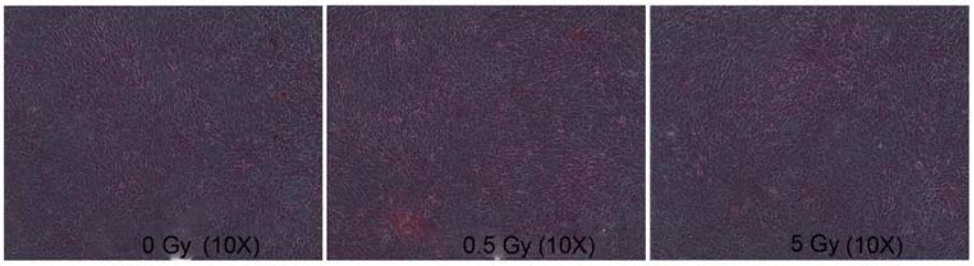

Figure 11. Alkaline phosphatase staining. Following alkaline phosphatase staining, the cytoplasm of osteoblasts was purple granular, and the staining was positive. Magnification, x10.

Cytoskeleton rearrangement occurred and was maintained for 5 days. Thus, the disordered cytoskeleton arrangement was hypothesized to be due radiation-induced damage, where an as yet unknown repair system had been activated causing F-actin rearrangement. These changes were similar to mechanical force-induced cytoskeleton reorganization (26). Additionally, Ricci *et al* (23) demonstrated that 0.5 Gy X-ray irradiation caused cytoskeleton reorganization and an increase in the number of stress fibers in the cytoplasm. However, the mechanisms involved in stimulating cellular signaling pathways during DNA damage repair remain to be elucidated. In the current study, F-actin expression post-irradiation decreased gradually in a time-dependent manner; however, at day 7 F-actin fluorescence intensity was similar to baseline, indicating that the cytoskeleton changes induced by 0.5 Gy X-ray were reversible. Furthermore, the F-actin cytoskeleton in MC3T3-E1 cells demonstrated decreased fluorescence intensity and disordered F-actin when irradiated by 5 Gy.

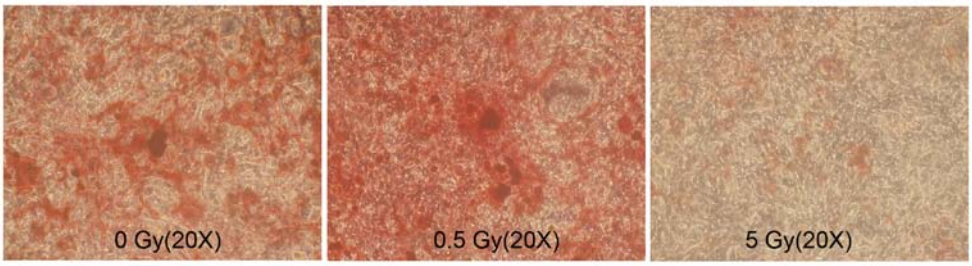

Figure 12. Alizarin red staining. Following alizarin red staining, multiple orange mineralized nodules of various sizes were observed. Magnification, x20.

The results of the current study demonstrated that the expression of RhoA, LIMK2, ROCK1 and p-cofilin increased during actin rearrangement following 0.5 Gy irradiation. These results provided evidence that RhoA/ROCK/LIMK2/cofilin constituted a pathway involved in the regulation of actin dynamics initiated by X-ray irradiation. These results were in accordance with a previous study by Rousseau *et al* (45). Furthermore, LIMK2 was linked to Rho GTPases and, via direct substrate cofilin, to actin microfilaments. A previous study demonstrated that Rho GTPases and their effector, ROCK1, were involved in MC3T3-E1 cells in response to flow shear stress, ultrasound and magnetic field (26). The results of the current study demonstrated the potential sequence of signaling as RhoGTPases regulating ROCK1, LIMK2 and cofilin to induce actin polymerization. However, the polymerization decreased on the 5th day post-irradiation as compared to the control group, which might be related to negative feedback regulation in the cells.

The current study demonstrated that the cofilin protein expression in the 0.5 and 5 Gy groups was higher than that in the non-irradiation group. X-ray irradiation was hypothesized to activate the Rho/ROCK pathway and increase the synthesis of P-cofilin, which was derived from the intracellular synthesis of cofilin. On days 3 and 5 following X-ray irradiation, the ratio of P-cofilin/cofilin increased significantly in the 0.5 Gy group, indicating that the synthetic cofilin was converted to P-cofilin. Additionally, the fluorescence intensity of F-actin decreased in cells pretreated with Y-27632. This further suggested that LDI-induced cytoskeleton remodeling may occur through the Rho/ROCK1/LIMK2/cofilin pathway.

Gabry *et al* (46) demonstrated that radiation causes rapid rearrangement of actin in capillary endothelial cells, leading to the activation the RhoA/ROCK signaling pathway. Rousseau *et al* (45) revealed that following 15 Gy X-ray irradiation, human microvascular endothelial cells exhibited cytoskeleton rearrangement and RhoA expression increased significantly. Previous studies have reported that 0.5 Gy LDI shrinks murine and bovine pulmonary capillary endothelial cells and increases intercellular space. These results were primarily attributed to the increase in actin depolymerization (28,47). Savla *et al* (44) demonstrated that bovine pulmonary artery endothelial cell permeability increased following 10 Gy irradiation, which disrupted the integrity of F-actin and that the number of incomplete actin crystals increased with the random distribution of F-actin in cells. Furthermore, Kantak *et al* (48) revealed that ionizing radiation induced the depolymerization of F-actin in vascular endothelial cells, increasing in a dose-dependent manner. These results may be related to cell type, cell sensitivity to radiation, culture environment and radiation dose.

The RhoA/ROCK signaling pathway is involved in the formation of the cytoskeleton, which promotes osteogenic differentiation by altering contact areas between the cells (49). Moreover, RhoGTPases are key mediators of the Wnt signaling pathway, which can influence cellular behavior through morphological and transcriptional changes (9). Therefore, the RhoA/ROCK signaling pathway may also interact with the Wnt signaling pathway, participating in LDI to promote osteoblast differentiation.

The initiating factor in ionizing radiation-induced RhoA activation has not been fully elucidated. Cells may produce large amounts of ROS following irradiation (50-52). RhoA has recently been discovered to be a target protein of reactive oxygen species (ROS) (53,54) ROS can activate multiple signaling pathways without ligand and receptor binding, thereby activating RhoA. Furthermore, ROS can activate stress-activated protein kinase (SAPK) family molecules, including SAPK2/p38, which cause endothelial cell cytoskeleton remodeling (55). Another putative pathway is the formation of sphingolipid ceramides on the cell membrane, which have been found to activate RhoA *in vitro* (56). Sphingolipid ceramindes act as critical messengers for transducing cellular stress (57). Additionally, Torroba *et al* (58) revealed that the activation of RhoA in epithelial cells requires a parallel signaling pathway involving the activation of phosphatidylinositol 3-kinase.

In conclusion, the results of the current study demonstrated that LDI caused reversible cytoskeleton reorganization. At a radiation dose of 5 Gy, MC3T3-E1 cells exhibited damaged cytoskeletons, and decreased and disorganized actin content. The RhoA/ROCK1/LIMK2/cofilin pathway may be a possible mechanism involved in these changes. Since cytoskeleton is closely associated with cell function, further research into the effects of LDI-induced actin reorganization on cell proliferation and differentiation is imperative.

Acknowledgements

Not applicable.

Funding

The current study was funded by the National Natural Science Foundation of China (grant no. 81171730). The funders did not have a role in study design, data collection, data analysis, decision to publish or the writing of the manuscript.

Availability of data and materials

The datasets used and/or analyzed during the current study are available from the corresponding author on reasonable request.

Authors' contributions

QH and ZZ conceived and coordinated the study, designed, performed and analyzed the experiments and wrote the paper. LW, WS, QX, XZ and LZ performed data collection, data analysis, and revised the paper. FY and QD designed the study, carried out the data analysis and revised the paper. All authors read and approved the final manuscript.

Ethics approval and consent to participate

Not applicable.

Patient consent for publication

Not applicable.

Competing interests

The authors declare that they have no competing interests.

References

1. Fazel R, Krumholz HM, Wang Y, Ross JS, Chen J, Ting HH, Shah ND, Nasir K, Einstein AJ and Nallamothu BK: Exposure to low-dose ionizing radiation from medical imaging procedures. N Engl J Med 361: 849-857, 2009.
2. Oh D and Huh SJ: Insufficiency fracture after radiation therapy. Radiat Oncol J 32: 213-220, 2014.
3. Michel G, Blery P, Pilet P, Guicheux J, Weiss P, Malard O and Espitalier F: Micro-CT analysis of radiation-induced osteopenia and bone hypovascularization in Rat. Calcif Tissue Int 97: 62-68, 2015.
4. Wei RL, Jung BC, Manzano W, Sehgal V, Klempner SJ, Lee SP, Ramsinghani NS and Lall C: Bone mineral density loss in thoracic and lumbar vertebrae following radiation for abdominal cancers. Radiother Oncol 118: 430-436, 2016.
5. Oest ME, Mann KA, Zimmerman ND and Damron TA: Parathyroid hormone (1-34) transiently protects against radiation-induced bone fragility. Calcif Tissue Int 98: 619-630, 2016.
6. Luckey T: Physiological benefits from low levels of ionizing radiation. Health Phys 43: 771-789, 1982.
7. Park SS, Kim KA, Lee SY, Lim SS, Jeon YM and Lee JC: X-ray radiation at low doses stimulates differentiation and mineralization of mouse calvarial osteoblasts. BMB Rep 45: 571-576, 2012.
8. Zhou XZ, Zhang G, Dong QR, Chan CW, Liu CF and Qin L: Low-dose X-irradiation promotes mineralization of fracture callus in a rat model. Arch Orthop Trauma Surg 129: 125-132, 2009.
9. Schlessinger K, Hall A and Tolwinski N: Wnt signaling pathways meet Rho GTPases. Genes Dev 23: 265-277, 2009.
10. Theocharopoulos N, Perisinakis K, Damilakis J, Papadokostakis G, Hadjipavlou A and Gourtsoyiannis N: Occupational exposure from common fluoroscopic projections used in orthopaedic surgery. J Bone Joint Surg Am 85: 1698-1703, 2003.
11. Pramojanee SN, Pratchayasakul W, Chattipakorn N and Chattipakorn SC: Low-dose dental irradiation decreases oxidative stress in osteoblastic MC3T3-E1 cells without any changes in cell viability, cellular proliferation and cellular apoptosis. Arch Oral Biol 57: 252-256, 2012.
12. Xu W, Xu L, Chen M, Mao YT, Xie ZG, Wu SL and Dong QR: The effects of low dose X-irradiation on osteoblastic MC3T3-E1 cells in vitro. BMC Musculoskelet Disord 13: 94, 2012.
13. Chen M, Huang Q, Xu W, She C, Xie ZG, Mao YT, Dong QR and Ling M: Low-dose X-ray irradiation promotes osteoblast proliferation, differentiation and fracture healing. PLoS One 9: e104016, 2014.
14. Murata K, Noda SE, Oike T, Takahashi A, Yoshida Y, Suzuki Y, Ohno T, Funayama T, Kobayashi Y, Takahashi T and Nakano T: Increase in cell motility by carbon ion irradiation via the Rho signaling pathway and its inhibition by the ROCK inhibitor Y-27632 in lung adenocarcinoma A549 cells. J Radiat Res 55: 658-664, 2014.
15. Chen M, Dong QR, Huang Q, Xu W and She C: Effects of 0.5 Gy X-ray radiation on the profile of gene expression in MC3T3-E1 osteoblasts. Zhonghua Yi Xue Za Zhi 96: 2659-2664, 2016 (In Chinese).
16. Kawano T, Zhu M, Troiano N, Horowitz M, Bian J, Gundberg C, Kolodziejczak K and Insogna K: LIM kinase 1 deficient mice have reduced bone mass. Bone 52: 70-82, 2013.
17. Szezerbaty SKF, de Oliveira RF, Pires-Oliveira DAA, Soares CP, Sartori D and Poli-Frederico RC: The effect of low-level laser therapy (660 nm) on the gene expression involved in tissue repair. Lasers Med Sci 33: 315-321, 2018.
18. Kurpinski K, Jang DJ, Bhattacharya S, Rydberg B, Chu J, So J, Wyrobek A, Li S and Wang D: Differential effects of x-rays and high-energy 56Fe ions on human mesenchymal stem cells. Int J Radiat Oncol Biol Phys 73: 869-877, 2009.
19. Li X, Liu C, Li P, Li S, Zhao Z, Chen Y, Huo B and Zhang D: Connexin 43 is a potential regulator in fluid shear stress-induced signal transduction in osteocytes. J Orthop Res 31: 1959-1965, 2013.
20. Moorer MC and Stains JP: Connexin43 and the intercellular signaling network regulating skeletal remodeling. Curr Osteoporos Rep 15: 24-31, 2017.
21. Gotlieb AI: The endothelial cytoskeleton: Organization in normal and regenerating endothelium. Toxicol Pathol 18: 603-617, 1990.
22. McBeath R, Pirone DM, Nelson CM, Bhadriraju K and Chen CS: Cell shape, cytoskeletal tension, and RhoA regulate stem cell lineage commitment. Dev Cell 6: 483-495, 2004.
23. Ricci R, Pazos MC, Borges RE and Pacheco-Soares C: Biomodulation with low-level laser radiation induces changes in endothelial cell actin filaments and cytoskeletal organization. J Photochem Photobiol B 95: 6-8, 2009.
24. Tani A, Chellini F, Giannelli M, Nosi D, Zecchi-Orlandini S and Sassoli C: Red (635 nm), Near-infrared (808 nm) and Violet-Blue (405 nm) photobiomodulation potentiality on human osteoblasts and mesenchymal stromal cells: A morphological and molecular in vitro study. Int J Mol Sci 19: 1946, 2018.
25. Zhang S, Cheng J and Qin YX: Mechanobiological modulation of cytoskeleton and calcium influx in osteoblastic cells by short-term focused acoustic radiation force. PLoS One 7: e38343, 2012.
26. Arnsdorf EJ, Tummala P, Kwon RY and Jacobs CR: Mechanically induced osteogenic differentiation-the role of RhoA, ROCKII and cytoskeletal dynamics. J Cell Sci 122: 546-553, 2009.
27. Kempf SJ, Buratovic S, von Toerne C, Moertl S, Stenerlöw B, Hauck SM, Atkinson MJ, Eriksson P and Tapio S: Ionising radiation immediately impairs synaptic plasticity-associated cytoskeletal signalling pathways in HT22 cells and in mouse brain: An in vitro/in vivo comparison study. PLoS One 9: e110464, 2014.
28. Onoda JM, Kantak SS and Diglio CA: Radiation induced endothelial cell retraction in vitro: Correlation with acute pulmonary edema. Pathol Oncol Res 5: 49-55, 1999.
29. Wang S, Chen C, Su K, Zha D, Liang W, Hillebrands JL, Goor Hv and Ding G: Angiotensin II induces reorganization of the actin cytoskeleton and myosin light-chain phosphorylation in podocytes through rho/ROCK-signaling pathway. Ren Fail 38: 268-275, 2016.
30. Etienne-Manneville S and Hall A: Rho GTPases in cell biology. Nature 420: 629-635, 2002.
31. Amano M, Nakayama M and Kaibuchi K: Rho-kinase/ROCK: A key regulator of the cytoskeleton and cell polarity. Cytoskeleton (Hoboken, NJ) 67: 545-554, 2010.
32. Tang AT, Campbell WB and Nithipatikom K: ROCK1 feedback regulation of the upstream small GTPase RhoA. Cell Signal 24: 1375-1380, 2012.
33. Carlier MF and Pantaloni D: Control of actin assembly dynamics in cell motility. J Biol Chem 282: 23005-23009, 2007.
34. Livak KJ and Schmittgen TD: Analysis of relative gene expression data using real-time quantitative PCR and the 2(-Delta Delta C(T)) method. Method 25: 402-408, 2001.

35. Vardouli L, Moustakas A and Stournaras C: LIM-kinase 2 and cofilin phosphorylation mediate actin cytoskeleton reorganization induced by transforming growth factor-beta. J Biol Chem 280: 11448-11457, 2005.
36. Zeng X, Feng Q, Zhao F, Sun C, Zhou T, Yang J and Zhan X: Puerarin inhibits TRPM3/miR-204 to promote MC3T3-E1 cells proliferation, differentiation and mineralization. Phytother Res 32: 996-1003, 2018.
37. Pollard TD and Goldman RD: Overview of the cytoskeleton from an evolutionary perspective. Cold Spring Harb Perspect Biol 10: a030288, 2018.
38. Blanquie O and Bradke F: Cytoskeleton dynamics in axon regeneration. Curr Opin Neurobiol 51: 60-69, 2018.
39. Wang Y, Shan Q, Pan J and Yi S: Actin cytoskeleton affects schwann cell migration and peripheral nerve regeneration. Front Physiol 9: 23, 2018.
40. Szymanski D and Staiger CJ: The actin cytoskeleton: Functional arrays for cytoplasmic organization and cell shape control. Plant Physiol 176: 106-118, 2018.
41. Galli C, Piemontese M, Lumetti S, Ravanetti F, Macaluso GM and Passeri GJ: Actin cytoskeleton controls activation of Wnt/β-catenin signaling in mesenchymal cells on implant surfaces with different topographies. Acta Biomater 8: 2963-2968, 2012.
42. Panzetta V, De Menna M, Musella I, Pugliese M, Quarto M, Netti PA and Fusco S: X-rays effects on cytoskeleton mechanics of healthy and tumor cells. Cytoskeleton (Hoboken, NJ) 74: 40-52, 2017.
43. Mohammadkarim A, Tabatabaei M, Parandakh A, Mokhtari-Dizaji M, Tafazzoli-Shadpour M and Khani MM: Radiation therapy affects the mechanical behavior of human umbilical vein endothelial cells. J Mech Behav Biomed Mater 85: 188-193, 2018.
44. Savla U and Waters CM: Barrier function of airway epithelium: Effects of radiation and protection by keratinocyte growth factor. Radiat Res 150: 195-203, 1998.
45. Rousseau M, Gaugler MH, Rodallec A, Bonnaud S, Paris F and Corre I: RhoA GTPase regulates radiation-induced alterations in endothelial cell adhesion and migration. Biochem Biophys Res Commun 414: 750-755, 2011.
46. Gabryś D, Greco O, Patel G, Prise KM, Tozer GM and Kanthou C: Radiation effects on the cytoskeleton of endothelial cells and endothelial monolayer permeability. Int J Radiat Oncol Biol Phys 69: 1553-1562, 2007.
47. Speidel MT, Holmquist B, Kassis AI, Humm JL, Berman RM, Atcher RW, Hines JJ and Macklis RM: Morphological, biochemical, and molecular changes in endothelial cells after alpha-particle irradiation. Radiat Res 136: 373-381, 1993.
48. Kantak SS, Diglio CA and Onoda JM: Low dose radiation-induced endothelial cell retraction. Int J Radiat Biol 64: 319-328, 1993.
49. Seo CH, Jeong H, Feng Y, Montagne K, Ushida T, Suzuki Y and Furukawa KS: Micropit surfaces designed for accelerating osteogenic differentiation of murine mesenchymal stem cells via enhancing focal adhesion and actin polymerization. Biomaterials 35: 2245-2252, 2014.
50. Cao X, Wu X, Frassica D, Yu B, Pang L, Xian L, Wan M, Lei W, Armour M, Tryggestad E, *et al*: Irradiation induces bone injury by damaging bone marrow microenvironment for stem cells. Proc Natl Acad Sci USA 108: 1609-1614, 2011.
51. Rodrigues-Moreira S, Moreno SG, Ghinatti G, Lewandowski D, Hoffschir F, Ferri F, Gallouet AS, Gay D, Motohashi H, Yamamoto M, *et al*: Low-dose irradiation promotes persistent oxidative stress and decreases self-renewal in hematopoietic stem cells. Cell Rep 20: 3199-3211, 2017.
52. Wang C, Blough E, Dai X, Olajide O, Driscoll H, Leidy JW, July M, Triest WE and Wu M: Protective effects of cerium oxide nanoparticles on MC3T3-E1 osteoblastic cells exposed to X-ray irradiation. Cell Physiol Biochem 38: 1510-1519, 2016.
53. Chu S, Mao X, Guo H, Wang L, Li Z, Zhang Y, Wang Y, Wang H, Zhang X and Peng W: Indoxyl sulfate potentiates endothelial dysfunction via reciprocal role for reactive oxygen species and RhoA/ROCK signaling in 5/6 nephrectomized rats. Free Radic Res 51: 237-252, 2017.
54. Luo J, Li D, Wei D, Wang X, Wang L and Zeng X: RhoA and RhoC are involved in stromal cell-derived factor-1-induced cell migration by regulating F-actin redistribution and assembly. Mol Cell Biochem 436: 13-21, 2017.
55. Aghajanian A, Wittchen ES, Campbell SL and Burridge K: Direct activation of RhoA by reactive oxygen species requires a redox-sensitive motif. PLoS One 4: e8045, 2009.
56. Truman JP, García-Barros M, Kaag M, Hambardzumyan D, Stancevic B, Chan M, Fuks Z, Kolesnick R and Haimovitz-Friedman A: Endothelial membrane remodeling is obligate for anti-angiogenic radiosensitization during tumor radiosurgery. PLoS One 5: e12310, 2010.
57. Shi F, Wang YC, Hu ZB, Xu HY, Sun J, Gao Y, Li XT, Yang CB, Xie C, Li CF, *et al*: Simulated microgravity promotes angiogenesis through RhoA-dependent rearrangement of the actin cytoskeleton. Cell Physiol Biochem 41: 227-238, 2017.
58. Torroba B, Herrera A, Menendez A and Pons S: PI3K regulates intraepithelial cell positioning through Rho GTP-ases in the developing neural tube. Dev Biol 436: 42-54, 2018.